AAC
Journals.ASM.org

# Discovery of Safe and Orally Effective 4-Aminoquinaldine Analogues as Apoptotic Inducers with Activity against Experimental Visceral Leishmaniasis

**Partha Palit,[a]* Abhijit Hazra,[b] Arindam Maity,[b] R. S. K. Vijayan,[c] Prabu Manoharan,[c] Sukdeb Banerjee,[b] Nirup B. Mondal,[b] Nanda Ghoshal,[c] and Nahid Ali[a]**

Infectious Diseases and Immunology Division, Indian Institute of Chemical Biology,[a] Steroid and Terpenoid Division, Indian Institute of Chemical Biology,[b] and Structural Biology and Bioinformatics Division, Indian Institute of Chemical Biology,[c] Kolkata, India

**Novel antileishmanials are urgently required to overcome emergence of drug resistance, cytotoxic effects, and difficulties in oral delivery. Toward this, we investigated a series of novel 4-aminoquinaldine derivatives, a new class of molecules, as potential antileishmanials. 4-Aminoquinaldine derivatives presented inhibitory effects on *L. donovani* promastigotes and amastigotes (50% inhibitory concentration range, 0.94 to 127 $\mu$M). Of these, PP-9 and PP-10 were the most effective *in vitro* and demonstrated strong efficacies *in vivo* through the intraperitoneal route. They were also found to be effective against both sodium antimony gluconate-sensitive and -resistant *Leishmania donovani* strains in BALB/c mice when treated orally, resulting in more than 95% protection. Investigation of their mode of action revealed that killing by PP-10 involved moderate inhibition of dihydrofolate reductase and elicitation of the apoptotic cascade. Our studies implicate that PP-10 augments reactive oxygen species generation, evidenced from decreased glutathione levels and increased lipid peroxidation. Subsequent disruption of *Leishmania* promastigote mitochondrial membrane potential and activation of cytosolic proteases initiated the apoptotic pathway, resulting in DNA fragmentation and parasite death. Our results demonstrate that PP-9 and PP-10 are promising lead compounds with the potential for treating visceral leishmaniasis (VL) through the oral route.**

The protozoan parasites of the genus *Leishmania* are the causative agents of the disease leishmaniasis (58). Epidemiological studies reveal that leishmaniasis is endemic in 88 countries, particularly in subtropical and tropical regions, and is estimated to afflict 12 million people worldwide (57). Leishmaniasis manifests mainly in three clinical forms: visceral leishmaniasis (VL), cutaneous leishmaniasis (CL), and mucocutaneous leishmaniasis (MCL). Clinical manifestations range from skin lesions, which are evident in CL, to clinical presentations of hepatosplenomegaly, which are evident in VL (8). VL causes large-scale mortality and morbidity among the poorest of the poor in the Indian subcontinent and Africa and is classified as a neglected disease by WHO and Medicines San Frontieres. There are no licensed vaccines, and chemotherapy is the mainstay to combat the disease. The armamentarium of drugs currently approved is limited to amphotericin B and its various liposomal formulations, paromomycin, and pentavalent antimonials. Miltefosine, the only oral drug approved for VL (10), cannot be used in children and pregnant women, as gastrointestinal toxicity and teratogenicity were evident from clinical trials carried out in India (22). The other drugs also suffer from shortcomings, such as unacceptable adverse effects, poor efficacy, limited accessibility due to high cost, and poor compliance, as they require parenteral administration and long treatment regimens (40). Additionally, the other compounding factors of concern are the emergence of drug resistance, particularly toward pentavalent antimonials in the Indian subcontinent (44), and resurgence of VL with HIV as a coinfection (48). Progress in antileishmanial drug discovery has been hampered due to the lack of a profitable drug market, which dampens serious attention from pharmacy majors, as leishmaniasis fails to qualify as a global disease (42). These issues emphasize an imperative need to carry out drug discovery programs that would significantly accelerate and facilitate the identification of novel and safer chemotherapeutic agents against leishmaniasis.

Earlier, our group synthesized a novel quinoline derivative (S-4), 2-(2-methylquinolin-4-ylamino)-*N*-phenylacetamide (47), which showed strong antiparasitic activity both *in vitro* and *in vivo* against *Leishmania donovani*. It was hypothesized that 4-aminoquinaldine compounds would retain antiparasitic activity, as multiple reports entail that quinoline scaffold-based derivatives, such as indolyl quinoline analogues (7), 4-substituted quinoline (19), 2-substituted quinoline (36), 8-amino quinoline derivatives (sitamaquine) (30), and 2 propylene quinoline derivatives (33), display antiparasitic activities. On the basis of informed rationality, nine 4-aminoquinaldines were synthesized by introducing numerous R groups at the 4 amino position of quinaldine scaffolds (14). In addition, two more compounds, PP-9 and PP-10, analogues of S-4, were synthesized by inserting two chlorine atoms at the anilide position of 4-aminoquinaldine moieties. Herein, these 11 compounds (Table 1) were tested against *L. donovani* parasites and their antileishmanial activities were evaluated in comparison with S-4.

Received 20 May 2011 Returned for modification 23 July 2011
Accepted 29 September 2011
Published ahead of print 24 October 2011
Address correspondence to Nahid Ali, nali@iicb.res.in.
* Present address: Dr. B. C. Roy College of Pharmacy and Allied Health Sciences, Bidhannagar, Durgapur, India.
Supplemental material for this article may be found at http://aac.asm.org/.

doi:10.1128/AAC.00700-11

**TABLE 1** Structure and nomenclature of the 4-aminoquinaldine derivatives

| Product | Structure | IUPAC name |
|---|---|---|
| S4 | 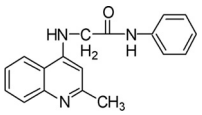 | 2-(2-Methyl-quinolin-4-ylamino)-*N*-phenyl-acetamide |
| PP-1 | 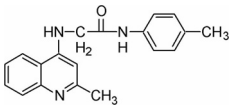 | 2-(2-Methyl-quinolin-4-ylamino)-*N*-*p*-tolyl-acetamide |
| PP-2 | 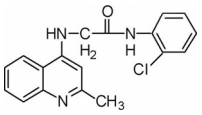 | *N*-(2-Chloro-phenyl)-2-(2-methyl-quinolin-4-ylamino)-acetamide |
| PP-3 | 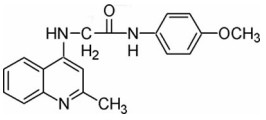 | *N*-(4-Methoxy-phenyl)-2-(2-methyl-quinolin-4-ylamino)-acetamide |
| PP-4 | 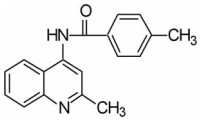 | 4-Methyl-*N*-(2-methyl-quinolin-4-yl)-benzamide |
| PP-7 | 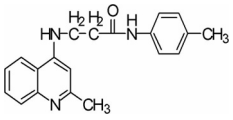 | *N*-(4-Methyl-phenyl)-3-(2-methyl-quinolin-4-ylamino)-propionamide |
| PP-8 | 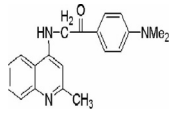 | 1-(4-Dimethylamino-phenyl)-3-(2-methyl-quinolin-4-ylamino)-propan-2-one |
| PP-9 | 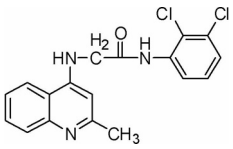 | *N*-(2,3-Dichloro-phenyl)-2-(2-methyl-quinolin-4-ylamino)-acetamide |
| PP-10 | 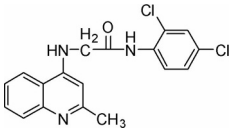 | *N*-(2,4-Dichloro-phenyl)-2-(2-methyl-quinolin-4-ylamino)-acetamide |
| PP-11 | 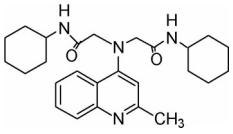 | *N*-Cyclohexyl-2-[cyclohexylcarbamoylmethyl-(2-methyl-quinolin-4-yl)-amino]-acetamide |
| PP-12 | 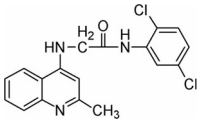 | *N*-(2,5-Dichloro-phenyl)-2-(2-methyl-quinolin-4-ylamino)-acetamide |
| PP-13 | 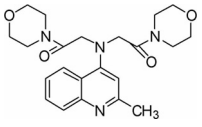 | 2-[(2-Methyl-quinolin-4-yl)-(2-morpholin-4-yl-2-oxo-ethyl)-amino]-1-morpholin-4-yl-ethanone |

In this series of compounds, PP-9 and PP-10 displayed the most pronounced activity against both sodium antimony gluconate (SAG)-sensitive and -resistant *L. donovani*. These compounds with impressive oral permeabilities demonstrated remarkable *in vivo* antileishmanial activity through the oral route. PP-10 elicited its antileishmanial activity through programmed cell death (PCD) involving upregulation of reactive oxygen species (ROS) generation (28), subsequent protease activation, and DNA fragmentation, coupled with moderate inhibition of leishmanial dihydrofolate reductase (DHFR).

## MATERIALS AND METHODS

**Chemistry.** Synthesis procedure and spectral data for all the experimental compounds except PP-9 and PP-10 were previously reported (14). PP-9 and PP-10 were synthesized by reacting dichloroacetyl chloride with 4-aminoquinaldine with substituted anilines in the presence of sodium hydride in dry dimethyl sulfoxide (DMSO) under a nitrogen atmosphere, giving rise to the products. Two compounds were separated by column chromatography over silica gel (60 to 120 mesh), eluting with different ratios of a chloroform-methanol mixture, and were characterized by the results of their spectroscopic analyses (infrared, $^{1}H$, $^{13}C$, and mass spectral). Chemical spectral data for PP-9 and PP-10 are given in the supplemental material.

**Chemicals.** All chemicals used in the experiments were of analytical grade and were procured from Sigma-Aldrich and E. Merck.

**Biology, parasite culture, and animals.** Promastigotes of *L. donovani* strain AG83 (MHOM/IN/1983/AG83) were maintained in golden hamsters and cultured at 22°C in medium 199 (M199) supplemented with 10% fetal calf serum (FCS), 100 IU/ml penicillin, and 100 mg/liter streptomycin (M119-FCS) (1). Another strain, GE1F8R, is an *in vitro*-developed SAG-resistant isolate originally obtained from a kala-azar patient (MHOM/IN/89/GE1F8R). Promastigotes of *L. major* (MHOM/SU/73/5-ASKH) were cultured in Dulbecco's modified Eagle medium (DMEM) at 22°C and maintained in BALB/c mice by serial passage. A green fluorescent protein (GFP)-transfected SAG-resistant parasite, a clinical isolate of *L. donovani* (GFP2039), was obtained from Central Drug Research Institute, India, and cultured in RPMI 1640 (Sigma) containing 25 mM HEPES, 40 μg/ml gentamicin supplemented with 10% FCS at 25°C. Four-week-old hamsters and BALB/c mice, reared in institute facilities, were used for the purpose of parasite maintenance and experimental work, respectively, with prior approval of the Animal Ethics Committee of the Indian Institute of Chemical Biology.

**Antileishmanial assays *in vitro* and *in vivo* on *L. donovani* parasites.** To investigate the antileishmanial effect of synthesized 4-aminoquinaldine derivatives (PP compounds) on promastigotes, freshly transformed promastigotes of *L. donovani* AG83 ($2 \times 10^6$/ml) in M199 containing 10% FCS were incubated with graded concentrations of PP compounds at 22°C for 2 h. After treatment, the parasites were centrifuged and subsequently washed with phosphate-buffered saline (PBS; 0.02 M). The pellets were resuspended in 100 μl PBS solution containing a 2-mg/ml concentration of dimethyl thiazolyl diphenyl tetrazolium salt (MTT). Their viability was determined in a spectrophotometer (Hitachi High Technologies) at 570 nm by measuring the optical density (OD) of reduced formazan (35), after incubation for 4 h at 22°C, compared to untreated cells. To investigate the effect of the synthesized derivatives on intracellular amastigotes, resident peritoneal macrophages ($10^6$ cells) isolated from BALB/c mice were infected with *L. donovani* AG83 promastigotes at a ratio of 1:10 at 37°C. Following infection for 6 h, the macrophages were treated for 48 h with different concentrations of PP compounds. The antileishmanial efficacy of these derivatives toward the intracellular amastigotes was evaluated through microscopic counting of the number of amastigotes per 200 macrophages by the Giemsa staining method (1, 15). All 50% inhibitory concentrations ($IC_{50}$s) of these derivatives against promastigotes and amastigotes were determined by linear regression from the percentages of killing compared to untreated vehicle controls (0.5% DMSO). The activities of the most potent compounds, PP-9 and PP-10, obtained from screening against AG83, were further tested on amastigotes of SAG-resistant strain GE1F8R and compared with the activity of miltefosine as described above.

The compounds S-4, PP-2, PP-9, and PP-10 for the *in vivo* evaluation on BALB/c mice against both SAG-sensitive and -resistant *L. donovani* parasites were selected on the basis of their activities against intracellular amastigotes. BALB/c mice were infected intravenously (i.v.) with $2 \times 10^7$ amastigotes isolated from spleens of infected hamsters. After 8 weeks of infection, the mice were treated either intraperitoneally (i.p.) or orally once a week for 1 month. Mice were sacrificed 2 days after the last treatment, and the parasite burdens of spleen and liver were estimated and expressed as Leishman Donovan units (LDUs) (41).

**Log $D_{7.4}$ and oral permeability determination of the two lead compounds, PP-9 and PP-10.** Octanol and PBS at a ratio of 1:1 by volume were taken in a flask and shaken mechanically for 24 h to presaturate PBS with octanol and octanol with PBS. These presaturated solvents were used for the present study. Four hundred microliters PBS containing 4 μl each of 25 mM PP-9 and PP-10 was allowed to undergo partitioning with different volumes of octanol (100, 150, 200, and 400 μl). After phase mixing by vigorous shaking for 2 h, phase separation was done by centrifugation at $1,509 \times g$ for 5 min, followed by 1 h standing undisturbed. The PBS layer was taken out. To 100 μl PBS an aliquot of 100 μl acetonitrile (ACN) was added and the absorbance of the sample, along with the absorbances of reference samples (400 μl PBS containing 4 μl of 25 mM compound plus 400 μl ACN), was measured. Five standard compounds were similarly studied to check the validity of the method. Log *D* estimated at pH 7.4, the logarithm of the concentration ratio of the compound in organic and aqueous phases, was modified as follows to avoid determination of the compound in organic phase: $\log \{[(OD_{Ref} - OD_{sample}) \times \text{vol octanol}]/(OD_{Ref} \times \text{vol PBS})\}$, where $OD_{Ref}$ and $OD_{sample}$ are the ODs of the reference sample and study sample, respectively, and vol is volume.

**PAMPA.** Millipore acceptor (catalog no. MATRNPS50) and donor (catalog no. MAIPN4510) plates were used for the parallel artificial membrane permeability assay (PAMPA). The artificial membrane was prepared by adding 5 μl of 1% egg lecithin in dodecane and plated into the donor wells. One hundred fifty microliters solution containing 250 μM PP-9 or PP-10 compound in PBS, pH 7.4 (5% DMSO), was added to the donor wells, and the donor plate was placed onto the acceptor plate containing 300 μl PBS at pH 7.4 and holding 5% DMSO, ensuring proper contact between membrane and acceptor liquid with no entrapped air bubbles. Incubation was carried out for 16 h at room temperature in a water-saturated chamber to avoid evaporation from donor wells. Such experimental conditions were chosen to check validity and acceptability. Acceptor samples of 250 μl were taken out after incubation, and the absorbance of each compound at the respective maximum λ was measured. To 200 μl acceptor, 100 μl donor solution was added and mixed properly, and this mixture was termed the "equilibrium." Absorbance of the equilibrium was also determined. Five standard compounds of different permeability (high, medium, low) were also similarly studied to establish a permeability ranking. The integrity of the artificial membrane was checked by a Lucifer yellow permeation study as reported earlier (20a).

The calculation was as follows: $\log P_e = \log[C \times -\ln(1 - OD_{acceptor}/OD_{equilibrium})]$, where $\log P_e$ is the log of the effective permeability and *C* is the effective concentration. *C* is equal to $(V_D \times V_A)/(V_D + V_A) \times \text{area (cm}^2) \times \text{porosity} \times \text{time (in seconds)}$, where $V_D$ is the volume of the donor (ml) and $V_A$ is the volume of the acceptor (ml).

**Toxicity evaluation in BALB/c mice.** A few parameters, such as specific enzyme levels related to normal liver, kidney, and cardiac functions, were chosen to determine the toxic effects of the compounds. Analysis in serum was done after administration of 4 repeat therapeutic doses of experimental compounds to 4- to 6-week-old naïve BALB/c mice for 4 consecutive weeks. To evaluate whether all treated compounds at therapeutic doses (10 mg/kg of body weight) were safe, the sera of normal mice

and mice treated with compounds PP-2, PP-8, PP-9, and PP-10 at 40, 50, 10, and 10 mg/kg body weight, respectively, were estimated for serum enzymes: serum glutamate pyruvate transaminase (SGPT), serum glutamate oxaloacetate transaminase (SGOT), alkaline phosphatase (ALP), lactate dehydrogenase (LDH), and creatine kinase (CK-MB). In addition, constituents like blood urea, blood cholesterol, and blood creatinine were also measured at 1 month posttreatment. The enzymes, urea, and creatinine were assayed using kits from Dr. Reddy's Laboratories (Hyderabad, India) following the manufacturer's protocol. Blood urea and cholesterol activity were expressed as mg/dl, whereas SGPT, SGOT, and ALP were expressed as IU/liter and blood creatinine was expressed as mg/liter.

**Inspection of parasite ultrastructure by TEM.** Transmission electron microscopy (TEM) of untreated cells and cells treated with the $IC_{50}$ dose of PP-10 was performed (9). *L. donovani* promastigotes were treated for 1.5 and 3.5 h with PP-10 at $IC_{50}$ doses. Briefly, cells were fixed in 3% glutaraldehyde in PBS, postfixed with 1% $OsO_4$ for 16 to 20 h, gradually dehydrated in ethanol, and finally embedded in Spurr resin (32). Thin-cut sections were stained with uranyl acetate and lead acetate and examined under a transmission electron microscope (model Tecnai G2 Spirit BioTwin FP 5018/40; FEI Company, Hillsboro, OR).

**Double staining with annexin V and PI.** Externalization of phosphatidylserine (PS) is a feature of metazoan apoptosis (2). Annexin V-fluorescein isothiocyanate (FITC) binds to externalized PS in the early stage of parasite apoptosis. Cells that did not stain for either annexin V or propidium iodide (PI) were considered healthy, those staining for annexin V only were taken to be apoptotic, and those staining for PI as well as annexin V were taken to be late apoptotic because entry of PI indicates plasma membrane disruption. Those staining with only PI and not annexin V were taken to be necrotic cells. Thus, to investigate the status of PP-10-treated promastigotes, binding of annexin V-FITC and PI of the parasites was carried out using an annexin V-FITC staining kit (Molecular Probes). Briefly, cells were treated with PP-10 for 1.5 and 2 h at $IC_{50}$ doses and for 3.5 h at the $IC_{90}$ dose and were double stained with FITC-conjugated annexin V and PI (10 $\mu$g/ml) after incubation for 15 min. Subsequently, cells were washed and resuspended in annexin V binding buffer. Labeled cells were visualized with the help of an E-600 Nikon fluorescence microscope using a 510- to 560-nm excitation filter block for red fluorescence of PI and a 440- to 480-nm filter block for green fluorescence of annexin V-FITC. The percentages of early apoptotic cells (annexin V-positive) as well as necrotic (PI-positive) cells were determined by counting 100 cells from each group under a fluorescence microscope.

**Measurement of ROS levels.** To monitor the level of ROS, several ROS-specific dyes that could distinguish among the different species were used. The cell-permeant probe $H_2$DCFDA (2,7-dichlorodihydrofluorescein diacetate), a nonpolar compound that readily diffuses into cells, where it is hydrolyzed to the nonfluorescent derivative dichlorodihydrofluorescein and thus trapped within, was used for detection. In the presence of a proper oxidant, this compound is oxidized to the highly fluorescent 2,7-dichlorofluorescein. Briefly, PP-10-treated cells ($10^7$ promastigotes) were resuspended in 500 $\mu$l of M199 and labeled with $H_2$DCFDA (2 $\mu$g/ml) for 15 min in the dark (17). Fluorimetric analyses at 507-nm excitation and 530-nm emission wavelengths were carried out in a Fluostar Optima spectrofluorometer (BMG Technologies, Offenburg, Germany). Data were obtained after subtraction of the basal fluorescence.

**Estimation of superoxide radical.** To estimate the level of superoxide anion, $10^7$ promastigotes were incubated with or without PP-10 at $IC_{50}$ doses for different time periods. The cells were then washed with PBS and resuspended in 100 $\mu$l PBS buffer. Ten microliters of each suspension was added to 1 ml of reaction mixture containing 50 mM sodium carbonate, 50 mM nitroblue tetrazolium (NBT), 0.1 mM EDTA, and 0.5% Triton X-100 (26). In a parallel set of reactions, 100 nM superoxide dismutase (SOD) was added to each of the reaction mixtures prior to addition of the respective cell suspension. The reduction of NBT to blue formazan and its inhibition by SOD indicate the generation of superoxide radical. Analysis was carried out at 560 nm in a Hitachi spectrophotometer.

**Measurement of GSH level.** The glutathione (GSH) level was measured by monochlorobimane (MCB) dye, which gives a blue fluorescence when bound to glutathione. *L. donovani* promastigotes ($2.5 \times 10^6$) were treated with or without PP-10 at different times. Cells were then pelleted down and lysed by cell lysis buffer according to the manufacturer's protocol (Apo Alert glutathione assay kit). Cell lysates were incubated with MCB (2 mM) for 3 h at 37°C. The decrease in glutathione levels in the extracts of the nonapoptotic and apoptotic cells was detected by a fluorometer at 395-nm excitation and 480-nm emission wavelengths (56).

**Measurement of total fluorescent lipid peroxidation product.** AG83 promastigotes ($10^7$) treated and untreated with PP-10 at the $IC_{50}$ dose for 1.5, 2, and 3.5 h were pelleted down and washed twice with PBS. The pellet was suspended in 2 ml of 15% sodium dodecyl sulfate (SDS) in PBS solution. The fluorescence intensities of the total fluorescent lipid peroxidation products obtained from the SDS-promastigote interaction were estimated (53) with excitation at 360 nm and emission at 430 nm. A parallel set of treated groups was incubated with butylated hydroxytoluene (BHT; 20 mM), a specific inhibitor of lipid peroxidation.

**$\Delta\psi_m$ determinations.** Mitochondrial membrane potential ($\Delta\psi_m$) was measured using the JC-1 probe as described previously (4, 6), with slight modifications. JC-1 is a cationic mitochondrial vital dye that is lipophilic and becomes concentrated in the mitochondria in proportion to the membrane potential; more dye accumulates in mitochondria with greater membrane potential. Therefore, the fluorescence of JC-1 can be regarded as an indicator of the relative mitochondrial energy state. The dye exists as a monomer at lower concentrations (emission, 530 nm, and green fluorescence) and forms J aggregates at higher concentrations (emission, 590 nm, and red fluorescence). Briefly, PP-10-treated cells were collected and incubated for 7 min with 10 $\mu$M JC-1 at 37°C and were subsequently washed and resuspended in medium. The suspensions were measured for fluorescence at two different wavelengths as mentioned above. The ratio of the reading at 590 nm and that at 530 nm was considered the relative $\Delta\psi_m$ value.

**Effect of protease inhibitors on PP-10-treated *L. donovani* promastigotes.** *L. donovani* promastigotes ($2.5 \times 10^6$) were treated with or without PP-10 for different time periods at $IC_{50}$ doses. Cells were then pelleted and lysed by cell lysis buffer as per the manufacturer's protocol (Calbiochem). Cell lysates were incubated with caspase buffers to detect CED3/CPP32 protease activities. Individual fluorogenic peptide substrate Leu–Glu–His–Asp–7-amino-4-trifluoromethyl coumarin (DEVD-AFC for CED3/CPP32) at 100 mM and 1× reaction buffer containing 100 mM dithiothreitol (DTT) were added to the corresponding cell lysates. In a parallel set of reactions, 1 $\mu$l of the CED3/CPP32 group of protease inhibitors VAD-fmk (Val-Ala-Asp-fluoromethylketone) was added to the reaction mixture prior to the addition of cell lysates. Released 7-amino-4-methyl coumarins (AFCs) were detected after incubation of these samples at 37°C for 2 h by a fluorometer with 400-nm excitation and 505-nm emission wavelengths.

**DNA ladder assays.** Genomic DNAs were isolated from promastigotes at 1.5 and 3.5 h after they were treated with PP-10 at $IC_{50}$ doses and untreated *L. donovani* AG83 promastigotes ($2.5 \times 10^6$) with an apoptotic DNA ladder kit (Roche Biochemicals). In parallel, similar protocols were followed to isolate DNA from promastigotes treated with camptothecin at 1.74 $\mu$g/ml as positive controls. All DNAs were electrophoresed (51) in a 1.5% agarose gel at 75 V for 2 h, stained with ethidium bromide, and photographed under UV illumination.

**DHFR inhibition assay in *L. donovani* and *L. major* promastigotes with 4-aminoquinaldine derivatives PP-2, PP-9, and PP-10.** We assayed the DHFR inhibition activity of three lead compounds (PP-2, PP-9, and PP-10) against *L. donovani* (MHOM/IN/1983/AG83) and *L. major* (MHOM/SU/73/5-ASKH) promastigotes, as well as crude DHFR enzyme extracts isolated from human peripheral blood mononuclear cells (PBMCs), as described earlier, with slight modifications (46), to establish that DHFR is a target for these compounds (24). *L. major* and *L. donovani* promastigotes ($10^9$/ml of buffer [10 mM sodium phosphate, pH 7.0, 1

mM DTT, 1 mM EDTA]) were sonicated and centrifuged (10,000 × *g* for 20 min), and the supernatants of the sonic extracts were loaded in cuvettes with 850 μl of a reaction mixture (60 mM sodium phosphate [pH 7.0], 40 μM NADPH, 40 μM dihydrofolic acid, 250 μM EDTA, 250 μM DTT) to which the 4-aminoquinaldine analogues were added at graded concentrations. After 5 min to allow the reactants to mix, the reaction was initiated by the addition of 150 μl of the supernatant of the sonic extract. One cuvette did not receive drug (positive control); one cuvette did not receive either drug or enzyme (negative control). Percent inhibition of leishmanial and human DHFR activity was determined with respect to the decrease of NADP hydride (NADPH) absorbance at 340 nm of compound-treated samples in a spectrophotometer (DU-8; Beckman Instruments). For human DHFR, crude enzyme extract was obtained from $8 \times 10^6$ mononuclear cells by standard Ficoll-Hypaque density gradient ultracentrifugation of peripheral blood, followed by freeze-thawing of the cells 3 times and centrifugation at 16,000 × *g* for 15 min. Supernatants containing the crude human DHFR were assayed after addition of PP-2, PP-9, and PP-10 as described above.

**Molecular docking.** The X-ray structure of human DHFR was retrieved from the Protein Data Bank (PDB; PDB accession no. 1U72), and the *L. major* DHFR structure was generously provided by D. A. Mathews (25) on request. Standard preprocessing techniques were employed on the raw PDB files. Protonation states for the titratable residues were assigned assuming a pH of 7.4. A restrained minimization that allows hydrogen atoms to be flexible and the heavy atoms to be fixed was carried out to remove bad contacts and improve H bond geometries. Protein preparation was carried out using an Insight II apparatus (Accelrys, San Diego, CA), and high-quality ligand structures were prepared using the protocol stated elsewhere (31, 55). To predict the binding modes of the molecules in question, the GOLD (Genetic Optimization for Ligand Docking) program, which uses a genetic algorithm to find appropriate docking arrangements, was used to probe the binding modes of PP-2, PP-9, and PP-10 ligands within the DHFR active site. The extent of the binding site was defined to include all residues within 10 Å from the cocrystallized methotrexate molecule. A genetic algorithm search setting of 100 dockings with 100,000 genetic algorithm operations per docking was employed. The early termination option was turned on. Binding affinity estimation was carried out using the chemscore function, followed by an interaction-based filtering. The docking procedure was validated beforehand using the *de facto* self-docking method.

**Statistical analysis.** The data are presented as means ± standard errors of the means (SEMs). Differences between two groups were analyzed for statistical significance by unpaired Student's *t* test using GraphPad Prism (version 4) software. Differences were considered significant when $P$ was $<0.05$. $IC_{50}$s for drug for the *in vitro* cytotoxicity assay in the cell culture proliferation system were determined by sigmoidal growth curve analysis using GraphPad Prism (version 4) software and are presented as means ± standard deviations of at least three independent determinations.

## RESULTS

**4-Aminoquinaldine compounds are effective against both SAG-sensitive and SAG-resistant *Leishmania* parasites in culture.** We determined the *in vitro* leishmanicidal activity of 4-aminoquinaldines (denoted PP) after 2 and 48 h exposure to *L. donovani* (AG83) promastigotes (Table 2). Of the series studies, PP-2, PP-8, PP-9, and PP-10 demonstrated potent activities, with half-maximal inhibition concentrations ($IC_{50}$s for 2 h) ranging from 1.52 to 2.73 μM. Growth inhibition studies (48 h) illustrated that PP-9 and PP-10 were stronger inhibitors of *L. donovani* promastigotes, with $IC_{50}$s of 0.50 and 0.47 μM, respectively. Furthermore, exposure to intracellular amastigotes for 48 h demonstrated that 4-aminoquinaldine derivatives PP-2, PP-9, and PP-10 have significant $IC_{50}$s of 1.47, 1.08, and 0.94 μM, respectively, without showing any toxicity on murine peritoneal macrophages (Table 2). PP-9 and PP-10 were also effective against intracellular amastigotes of SAG-resistant *L. donovani* strains exhibiting $IC_{50}$s of 6.44 and 3.91 μM, respectively, for GFP2039 and 7.7 and 5.84 μM, respectively, for GE1F8R (Table 3). The $IC_{50}$ of PP-10 is 1.54-fold less than that of miltefosine against GE1F8R strains. Moreover, a significant reduction in green fluorescence of intracellular GFP2039 *L. donovani* amastigotes after PP-10 treatment at the $IC_{50}$ dose in contrast to that for untreated controls was observed (see Fig. 2C).

**Lead compounds are highly effective *in vivo* against murine model of VL.** Potent compounds were selected for assessment of antileishmanial activity in 8-week-old *L. donovani*-infected BALB/c mice. Compounds were administered i.p. once a week for 4 consecutive weeks. PP-9 and PP-10 were dosed at 10 mg/kg body weight, while PP-2 and PP-8 were given at 40 mg/kg during the course of treatment. The therapeutic doses of all the compounds were chosen to be 1/10 the 50% lethal dose ($LD_{50}$; acute toxicity) in BALB/c mice. Both PP-9 and PP-10 led to clearance of the parasite burden by 95% and 97% ($P < 0.0001$), respectively, in liver and 98% and 98.5% ($P < 0.0001$), respectively, in spleen at 30 days posttreatment in comparison to untreated controls. Mice treated with PP-2 and PP-8 exhibited 95.5% and 95% ($P < 0.0001$) reductions in the parasite burden in the liver, respectively, and 96.46% and 96% ($P < 0.0001$) reductions in the spleen, respectively, at 4-fold higher doses than PP-9 and PP-10 (Fig. 1a). PP-9 and PP-10 were then selected for oral administration at 10 mg/kg body weight. Both the compounds exhibited remarkable efficacy against both SAG-sensitive (AG83) (Fig. 1b) and SAG-resistant (GE1F8R) (Fig. 1c) strains. PP-9 and PP-10 suppressed the infection by 88% and 93%, respectively, in the liver, and 96% and 98% ($P < 0.0001$), respectively, in the spleen in AG83-infected mice at 4 weeks posttreatment (Fig. 1b). Furthermore, PP-9 and PP-10 could also clear the parasite burden by 94% and 97.46%, respectively, in the spleen ($P < 0.0001$) and 82% and 91%, respectively, in the liver ($P < 0.0001$) in SAG-resistant, *L. donovani* GE1F8R-infected BALB/c mice (Fig. 1c). In AG83- and GE1F8R-infected mouse models, oral administration of miltefosine at 10 mg/kg demonstrated 95% and 90.2% protection, respectively, in the spleen and 92% and 89% protection, respectively, in the liver. The leishmanicidal activity in the spleen elicited by PP-10 against both the strains was found to be better ($P < 0.05$) than that of miltefosine at equivalent dosages (10 mg/kg). In AG83- and GE1F8R-infected BALB/c mice, the parent compound, S-4, showed 4 and 16 times lower activity, respectively, in liver ($P < 0.05$) and 4.7 and 20 times lower activity, respectively, in spleen ($P < 0.05$) than PP-10. Notably, these results for S-4 were observed at a dose 5 times higher than that of PP-10 (Fig. 1b and c). At the therapeutic doses, none of the experimental compounds demonstrated any overt sign of clinical toxicity related to liver, kidney, or heart dysfunction posttreatment in healthy mice. The animals seemed to be completely healthy throughout the course of the experiment at posttreatment, with no variation in normal body weight. The spleen weights of the treated groups were significantly reduced compared to untreated controls in both intraperitoneal and oral therapy (data not shown).

**Physicochemical properties and permeability.** The $pK_a$ and log *P* values for all experimental compounds were determined using the software Cerius 2, version 4.10. Compound $pK_a$ values were evaluated by applying Chemaxon software (Table 4). The

**TABLE 2** 4-Aminoquinaldine analogues tested against *L. donovani* AG83 promastigotes for 2 and 48 h with their experimental $IC_{50}$ values

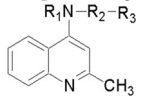


| Compound | Substituent | | | $IC_{50}$ ($\mu$M)[a] | | | |
|---|---|---|---|---|---|---|---|
| | $R_1$ | $R_2$ | $R_3$ | Experimental (2 h), promastigotes | Experimental (48 h), promastigote growth inhibition | Intracellular amastigotes | Murine peritoneal macrophage |
| S-4 | H | 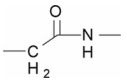 | 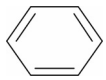 | 30.76 ± 1.14 | 10.72 ± 0.44 | 17 ± 2.21 | 250 ± 4.51 |
| PP-1 | H | 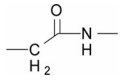 | 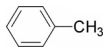 | 3.05 ± 0.34 | 1.31 ± 0.12 | 2.52 ± 0.31 | 100 ± 3.41 |
| PP-2 | H | 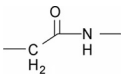 | 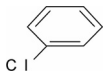 | 2.46 ± 0.26 | 0.62 ± 0.012 | 1.47 ± 0.13 | 98 ± 2.57 |
| PP-3 | H |  |  | 27 ± 1.76 | 6.60 ± 0.84 | 14.65 ± 1.03 | 174 ± 6.33 |
| PP-4 | H |  |  | 12.90 ± 0.91 | 3.48 ± 0.34 | 5.87 ± 0.73 | 225 ± 8.47 |
| PP-7 | H | 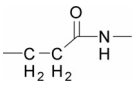 |  | 2.98 ± 0.36 | 0.75 ± 0.04 | 2.1 ± 0.23 | 125 ± 8.47 |
| PP-8 | H | 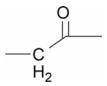 | 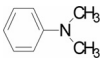 | 2.73 ± 0.16 | 0.72 ± 0.02 | 1.72 ± 0.08 | 165 ± 11.47 |
| PP-9 | H | 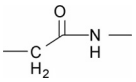 | 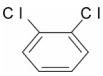 | 1.75 ± 0.06 | 0.50 ± 0.01 | 1.08 ± 0.04 | 92 ± 1.01 |
| PP-10 | H | 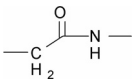 | 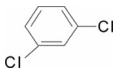 | 1.52 ± 0.03 | 0.47 ± 0.01 | 0.94 ± 0.01 | 90 ± 0.61 |
| PP-11 | 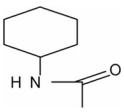 | 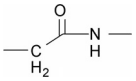 | 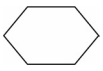 | 12.80 ± 0.93 | 5.62 ± 0.94 | 7.92 ± 0.94 | 190 ± 8.77 |
| PP-12 | H | 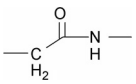 | 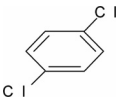 | 2.39 ± 0.13 | 2.17 ± 0.53 | 1.48 ± 0.26 | 88 ± 1.06 |
| PP-13 | 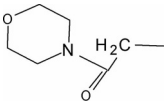 |  |  | 127.34 ± 1.93 | 89.27 ± 1.71 | 78 ± 1.71 | 240 ± 9.68 |

[a] All $IC_{50}$s are represented as means ± standard deviations of at least three independent determinations.

**TABLE 3** *In vitro* screening of activities of two potent compounds against sodium antimony gluconate-resistant *L. donovani* GE1F8R amastigotes and results of their inhibition of leishmanial and human DHFRs from cell supernatants and the docking study

| Compound | $IC_{50}$ ($\mu$M)[c] | | | | | | |
|---|---|---|---|---|---|---|---|
| | Experimental SAG-resistant amastigotes | | *Leishmania donovani* DHFR | *Leishmania* major DHFR | Human PBMC DHFR | Selectivity index | Chem score docking |
| | GE1F8R | GFP2039 | | | | | |
| PP-2 | ND[d] | ND | 3.38 ± 0.14 | 4.30 ± 0.14 | 49.85 ± 0.9 | 14.74,[a] 11.59[b] | 32.2102 |
| PP-9 | 7.7 ± 0.4 | 6.44 ± 0.24 | 1.67 ± 0.04 | 1.25 ± 0.01 | 14.44 ± 0.64 | 8.67,[a] 11.55[b] | 32.8070 |
| PP-10 | 5.84 ± 0.1 | 3.91 ± 0.13 | 1.11 ± 0.02 | 1.05 ± 0.01 | 13.34 ± 0.57 | 12.01,[a] 12.70[b] | 33.2650 |
| Miltefosine | 9.0 ± 0.60 | ND | ND | ND | ND | ND | ND |

[a] Selectivity for *L. donovani* (AG83) DHFR.
[b] Selectivity for *L. major* (5-ASKH) DHFR.
[c] Vales are means ± standard deviations of at least three independent determinations.
[d] ND, not determined.

most active compounds had a weakly basic $pK_a$ value of 8.71. Furthermore, both PP-9 and PP-10 were moderately lipophilic at physiologic pH, with log $D_{7.4}$ values of 0.91 and 0.97, respectively (Table 5). Moreover, PP-9 and PP-10 were highly permeant across the PAMPA Millipore membrane filter paper, showing permeation comparable to the permeations of the standard highly permeant drugs verapamil and diltiazem. The most potent compound, PP-10, exhibited 7-fold higher permeation than the standard oral antileishmanial drug, miltefosine (Table 5).

**Lead compound (PP-10) treatment induces morphological changes in *Leishmania* promastigote cells.** Electron microscopic studies on the ultrastructure of PP-10-treated *L. donovani* promastigotes at $IC_{50}$ doses showed that PP-10 induced certain morphological changes compared to untreated controls. The flagellated promastigotes lost their flagella, turned round with an increase in granules, vacuoles, and lipid bodies, and had fragmented cell nuclei at 1.5 h posttreatment (Fig. 2Ac and d). Parasites having condensed cytoplasm and dilated mitochondria and lacking kinetoplast DNA were observed following 1.5 h treatment with PP-10. Cells treated with PP-10 for 3.5 h lost their specialized membrane structures, showing increased dilation of the mitochondrial matrix and disruption of all internal cellular organelles (Fig. 2Ae) at late apoptotic stage due to exhibition of some necrotic cells in fluorescence microscopic images, as shown in Fig. 2Bc. We demonstrated PS exposure in the PP-10-treated promastigotes by annexin V labeling (Fig. 2B) and categorized the cells according to staining pattern, as described under Materials and Methods. It was found that after 1.5 h PP-10 treatment showed many annexin V-labeled cells (Fig. 2Bb) compared to untreated controls, where no annexin V-bound cells were observed. Exposure of promastigotes to the $IC_{50}$ dose of PP-10 for 2 h resulted in both annexin V- and PI-positive cells (Fig. 2Bc). Furthermore, treatment with the $IC_{90}$ dose of PP-10 for 3.5 h resulted in cells devoid of annexin V positivity and PI-positive cells. PS is usually confined to the inner leaflet of the cell membrane and is externalized when the cell is committed to apoptosis (49). These results therefore indicate that early and late apoptosis occurred at 1.5 and 2 h, respectively, after treatment at the $IC_{50}$ dose of PP-10. Treatment with PP-10 at $IC_{50}$ doses for 1.5 and 2 h produced 33% and 17% apoptotic (annexin V-positive) cells at early apoptotic and late apoptotic phases of promastigote cell death, respectively. In contrast, 8% and 31.4% necrotic cells (PI positive) were observed at 2 h and 3.5 h posttreatment with PP-10 at $IC_{50}$ and $IC_{90}$ doses, respectively.

**ROS generation caused by oxidative stress influences depletion of the glutathione (GSH) level and increases the level of lipid peroxidation.** *L. donovani* promastigotes were treated with the $IC_{50}$ dose of PP-10 to investigate the generation of ROS. The increase in the fluorescence intensity of the treated cells in comparison to untreated controls (0.2% DMSO) demonstrates that the $IC_{50}$ dose of PP-10 induces early apoptosis for up to 1.5 h due to the physiological production of ROS by the mitochondrion (Fig. 3Aa). After 2 h of treatment, the levels of ROS significantly declined with increasing time. Oxidative burst by enhancing the reactivity of ROS is an early event that also happened after PP-10 treatment and reached a peak value at about 1.5 h. Considering that oxidative burst occurs for a very short time (11), it seems that ROS acts as a trigger in PP-10-induced early apoptotic PCD, as reported by other investigators (12, 16, 51).

Cellular stress induced by PP-10 led to the formation of intracellular superoxide radicals, as evident by the reduction of NBT to blue formazan in the promastigote cell lysates. Superoxide radical levels in PP-10-treated cells remained 3.2- to 3.8-fold higher than the levels of controls throughout the experiment (Fig. 3Ab). After addition of SOD to the respective PP-10-treated cells, the intensity in the reduction of NBT to blue formazan by the lysates was inhibited by 85 to 90% at different times of incubation, confirming that the reduction of NBT is due to the formation of superoxide radicals.

GSH is a crucial molecule for protecting kinetoplastids from ROS and other free radicals (18). PP-10 caused a 35% reduction in GSH level after 1.5 h, and the consequence was enhanced to 56 and 62% at 2 and 3.5 h posttreatment, respectively (Fig. 3Ac).

Lipid peroxidation was quantified by measuring the total fluorescent lipid peroxide products in promastigotes after treatment with PP-10 at different time points, and the results demonstrated their upregulation at 1.5 h posttreatment, which reached a maximum level at 3.5 h. In the presence of 20 mM BHT, a specific inhibitor of lipid peroxidation, fluorescence levels dropped significantly, as observed in Fig. 3Ad. Hence, the ROS generation caused by PP-10-induced oxidative stress influenced depletion of the GSH level and increased the level of lipid peroxidation.

**PP-10 causes disruption of the mitochondrial membrane potential.** The BD MitoSensor JC-1 dye is a cationic mitochondrial vital dye that is lipophilic and becomes concentrated in the mitochondria in proportion to the level of depolarization of the membrane potential; more dye accumulation in mitochondria indicates the disruption of $\psi_m$. Herein, $\psi_m$ was expressed as the ratio of fluorescence at 590 nm/530 nm in response to PP-10 treatment.

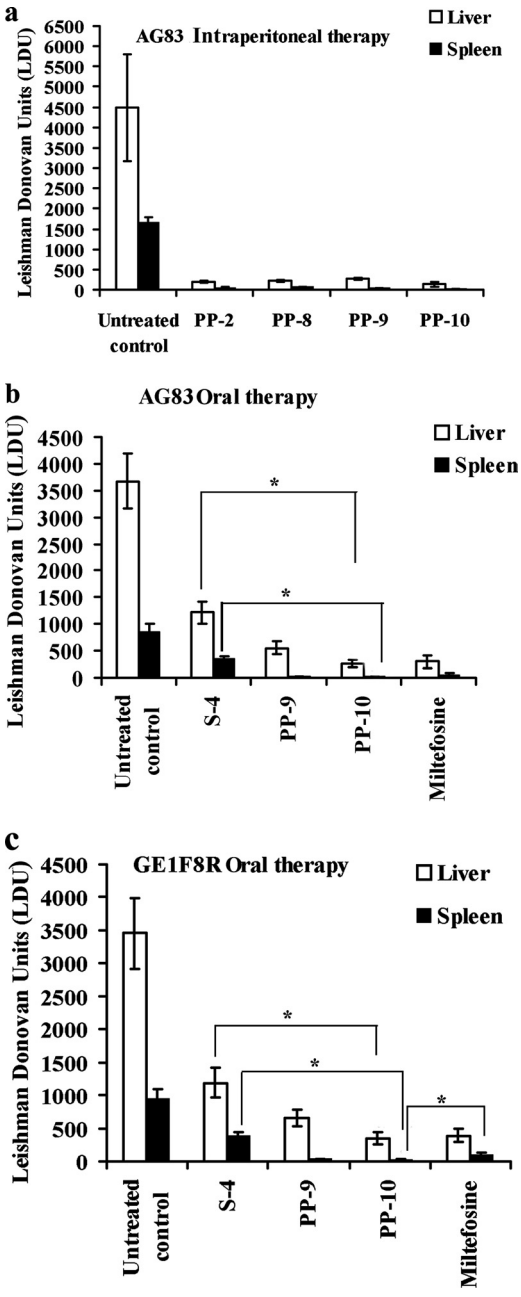


**FIG 1** Antileishmanial efficacy of 4-aminoquinaldine analogs in infected BALB/c mice. (a) In vivo antiparasitic activity of PP-2, PP-8, PP-9, and PP-10 administered through intraperitoneal route at doses of 40, 50, 10, and 10 mg/kg body weight, respectively, to AG83-infected (age, 8 weeks) BALB/c mice once a week for 4 consecutive weeks. (b) Mice infected with AG83 for 8 weeks were treated orally with PP-9, PP-10, and miltefosine at a dose of 10 mg/kg and S-4 at 50 mg/kg. Drugs were formulated in 0.1% Tween 80 and 0.5% methylcellulose in PBS solution and administered once a week for 1 month. (c) Mice infected with GE1F8R for 8 weeks were treated orally with PP-9, PP-10, and miltefosine at a dose of 10 mg/kg and S-4 at 50 mg/kg once a week for 4 consecutive weeks. Control infected animals received only 0.1% Tween 80 and 0.5% methylcellulose in PBS solution. Data represent the mean ± SEM ($n = 5$ mice per group) and are representative of three similar experiments. *, statistically significantly difference ($P < 0.05$) by comparison between two groups, assessed by the two-tailed unpaired Student *t* test.

PP-10 treatment at $IC_{50}$ doses for 1.5, 2, and 3.5 h demonstrated a progressive loss of the fluorescence ratio for the mitochondrial membrane potential by 37%, 50%, and 79% ($P < 0.0001$), respectively, with respect to untreated controls (Fig. 3Ba). Results show that PP-10 treatment led to collapse of the mitochondrial membrane potential and subsequently provoked cellular stress in response to changes in $\psi_m$.

**PP-10 causes activation of proteases in cytosol and DNA fragmentation.** Caspase-like protease, a member of the CED-3/CPP32 group of proteases, was measured fluorimetrically using its specific substrate Asp–Glu–Val–Asp–7-amino-4-trifluoromethyl coumarin (DEVD-AFC) in terms of liberated 7-amino-4-trifluoromethyl coumarin (AFC). PP-10 treatment significantly increased the activation of protease in AG83 promastigotes in a time-dependent manner compared to untreated controls (Fig. 3Bb). The activity of protease was reduced when cells were pretreated with the protease inhibitor VAD-fmk. This protease is a caspase-like protease, such as a metacaspase protein, for instance, calpains and cathepsins (CED3/CPP32 group of cysteine proteases), as *Leishmania* lacks a caspase gene. VAD-fmk, an irreversible inhibitor of the CED3/CPP32 group of proteases, may also inhibit these cysteine proteases, with activity being reduced to basal levels. Hence, such protease activation may also induce apoptotic cell death (12, 51).

Agarose gel electrophoresis at 37°C showed DNA ladder formation *in vitro* (Fig. 3Bc, lane 3) in isolated nuclei obtained from log-phase culture of leishmanial cells treated with PP-10 at the $IC_{50}$ dose for 2 h. The effect of fragmentation became more marked at 3.5 h posttreatment (lane 2). The cleavage patterns of genomic DNA characterized by fragmentation are typical of internucleosomal DNA digestion by an endogenous nuclease and a hallmark of apoptosis. Taken together, these results support the suggestion that PP-10 causes activation of proteases in the cytosol and genomic DNA fragmentation, which may contribute to the induction of apoptosis-like death of *L. donovani* parasites.

**Inhibition of leishmanial dihydrofolate reductase by potent compounds.** Spectrophotometric investigation of DHFR activity of sonicated supernatant derived from *L. donovani* (AG83) and *L. major* (5-ASKH) promastigotes at posttreatment with compounds at graded concentrations revealed that PP-2, PP-9, and PP-10 inhibited the AG83 DHFR at $IC_{50}$s of 3.38, 1.67, and 1.11 $\mu$M, respectively, and 5-ASKH DHFR at $IC_{50}$s of 4.30, 1.25, and 1.05 $\mu$M, respectively (Table 3). This inhibition correlated with the *in vitro* antileishmanial activity of the compounds. Although the highest concentration of these compounds inhibited the leishmanial DHFR to levels ranging from 70% to 84%, PP-2, PP-9, and PP-10 had weaker inhibitory activities on human PBMC-derived DHFR, with $IC_{50}$s of 49.85, 14.44, and 13.34 $\mu$M, respectively (Table 3).

**Molecular docking and binding studies.** Docking of PP-10, PP-9, and PP-2 into the active site of *L. major* DHFR revealed similar interaction patterns, in accordance with the cocrystal structure of methotrexate. A recent homology modeling and docking study (31) on *L. donovani chagasi* DHFR revealed that the *L. donovani chagasi* DHFR binding site is identical to that of the *L. major* DHFR and the protein-ligand interaction pattern is conserved in both species, suggesting that *L. major* DHFR can be used as a surrogate model for *L. donovani* DHFR-targeted drug discovery. The docked conformation of PP-10 revealed that the protonated nitrogen atom present in the 4-aminoquinaldine ring is involved in a hydrogen-bonding interaction with Val 156. The NH

**TABLE 4** Overview of physicochemical characteristics of novel 4-aminoquinaldine analogues

| Name | Melting point (°C) | State/form | Optical activity | $pK_a$[b] | Log *P*[c] | Mol wt | Color | Taste | Molecular formula | Solubility |
|---|---|---|---|---|---|---|---|---|---|---|
| S-4[a] | 220 | Solid amorphous powder | Nil | 8.71 | 0.970 | 291 | White | Bitter | $C_{18}H_{17}N_3O$ | Highly soluble in DMSO, acetonitrile, methanol, chloroform, and alcohol and sparingly soluble in water |
| PP-1 | 229 | -DO-[d] | -DO- | 8.71 | 1.470 | 305 | White | Bitter | $C_{19}H_{19}N_3O$ | -DO- |
| PP-2 | 178 | -DO- | -DO- | 8.71 | 1.690 | 325 | White | Bitter | $C_{18}H_{16}ClN_3O$ | -DO- |
| PP-3 | 217 | -DO- | -DO- | 8.72 | 1.040 | 321 | Reddish brown | Bitter | $C_{19}H_{19}N_3O_2$ | -DO- |
| PP-4 | 138 | -DO- | -DO- | 5.31 | 1.610 | 276 | White | Bitter | $C_{18}H_{16}N_2O$ | -DO- |
| PP-7 | 242 | -DO- | -DO- | 8.75 | 1.280 | 335 | Reddish brown | Bitter | $C_{20}H_{21}N_3O_2$ | -DO- |
| PP-8 | 210 | -DO- | -DO- | 8.71 | 1.160 | 333 | Grayish yellow | Bitter | $C_{20}H_{21}N_3O$ | -DO- |
| PP-9 | 235 | -DO- | -DO- | 8.71 | 2.350 | 360 | Reddish brown | Bitter | $C_{18}H_{15}Cl_2N_3O$ | -DO- |
| PP-10 | 215 | -DO- | -DO- | 8.71 | 2.130 | 360 | White | Bitter | $C_{18}H_{15}Cl_2N_3O$ | -DO- |
| PP-11 | 185 | Solid crystalline | -DO- | 8.58 | 2.770 | 436 | White | Bitter | $C_{26}H_{36}N_4O_2$ | -DO- |
| PP-12 | 227 | Solid amorphous powder | -DO- | 8.71 | 2.350 | 360 | White | Bitter | $C_{18}H_{15}Cl_2N_3O$ | -DO- |
| PP-13 | 221 | Solid crystalline | -DO- | 8.58 | −2.590 | 412 | White | Bitter | $C_{22}H_{28}N_4O_4$ | -DO- |

[a] S-4 is the parent compound from which the different analogues were generated by modifying the substituents.
[b] Compound $pK_a$ value was evaluated by applying Chemaxon software.
[c] Log *P* values are evaluated by using the software Cerius 2, version 4.10.
[d] -DO-, same as observed for S-4.

group attached to the phenyl ring forms a hydrogen-bonding interaction with Met 53, and the other NH group attached to the quinaldine ring is involved in an NH-$\pi$ interaction with Phe 56, as shown in Fig. 4A. The dichlorophenyl ring is involved in a T-stacking interaction with Phe 91, while the conformationally rigid quinaldine moiety is involved in a $\pi$-$\pi$ stacking interaction with Phe 56. The chlorine atom substituted at position 3 of the phenyl moiety (in PP-9) is involved in a weak halogen-mediated hydrogen-bonding interaction with Arg 97 (data not shown). Interestingly, the lead compounds PP-10, PP-9, and PP-2 exhibited significant differences in binding modes toward human DHFR, as shown in Fig. 4B (for PP-10). To counter the deficiencies in the scoring function, which fails to reflect the trend in selectivity, manual inspection of the difference in the binding mode was carried out and revealed that the lead compounds entail contact with two nonconserved amino acids (Met 53 and Phe 91) present in *L. major* DHFR (60), which apparently explains the selectivity for *L. major* DHFR over human DHFR. The considerable difference in the binding mode of PP-10 to *L. major* DHFR and human DHFR is evident from Fig. 4C and D, respectively. The selectivity profiles of these compounds are also evident from the results of spectrophotometric assays provided in Table 3.

## DISCUSSION

This is the first report of synthesized analogues of 4-aminoquinaldine with chlorine substituents with activity against exper-

**TABLE 5** Log *D* and permeability assay of PP-10 along with a few quality control samples

| | Log $D_{7.4}$ octanol/PBS | | Permeation of PP-9 and PP-10 and highly permeant drugs[a] | |
|---|---|---|---|---|
| Compound | Result | Reported value | Compound | PAMPA $P_e$ ($10^{-6}$ cm/s)[b] |
| Verapamil HCl | 2.29 | 2.42 | Verapamil | 13 |
| Propranolol HCl | 1.11 | 1.23 | Diltiazem | 9.2 |
| Metoprolol Tartrate | −0.27 | −0.30 | PP-9 | 8 |
| Furosemide | −1.13 | −1.28 | PP-10 | 11 |
| PP-9 | 0.91 | | Miltefosine | 1.78 |
| PP-10 | 0.97 | | Warfarin | 1.66 |
| | | | Methotrexate | 0.122 |

[a] Assessed by PAMPA at pH 7.4.
[b] Results are averages of two experiments.

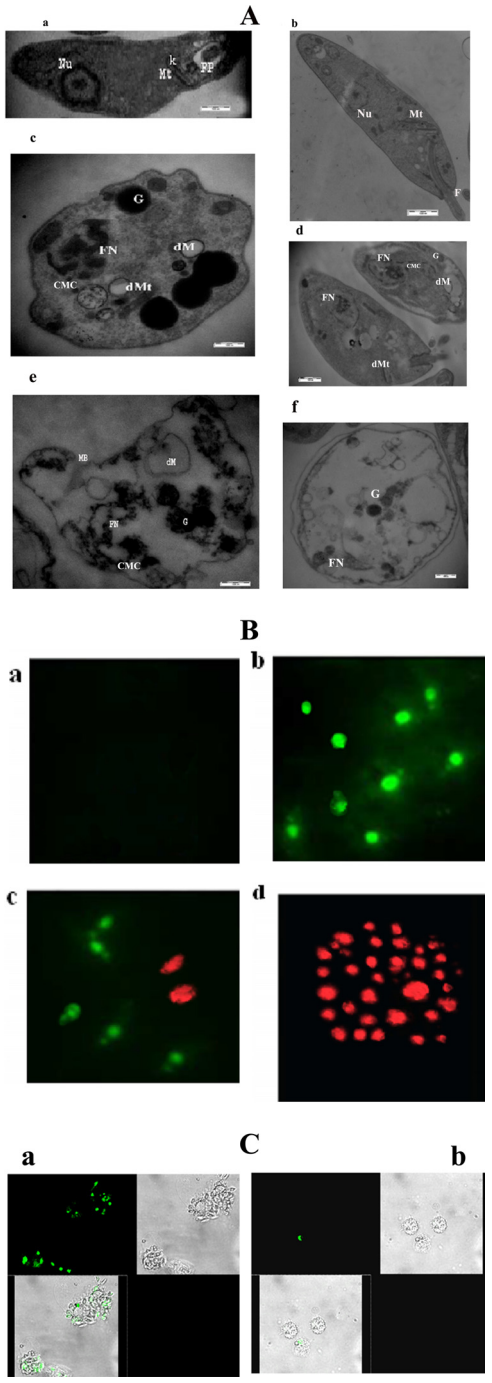


**FIG 2** Fluorescence microscopic analysis and ultrastructural changes of in vitro cytotoxicity of PP-10-treated cultured *L. donovani* promastigotes. (A) Electron microscopy of PP-10-treated and untreated AG83 promastigotes. Spurr blocks were prepared as described in Materials and Methods. Promastigotes were treated with 0.2% DMSO alone (a and b) or with $IC_{50}$ dose of PP-10 for 1.5 h treatment (c and d) or 3.5 h treatment (e and f). Magnifications, ×35,000 (a and b) and ×60,000 (c to f). Nu, nucleus; Mt, mitochondria; FP, flagellar pocket; k, kinetoplast; G, granules; FN, fragmented nuclei; dM, dilated matrix of mitochondria; dMt, dilated mitochondria; MB, membrane blabbing; CMC, condensed and marginated chromatin. Pictures are representative from one of three similar studies. (B) Phosphatidylserine exposure on promastigotes occurs after treatment with PP-10 at $IC_{50}$ dose. (a) Untreated control cells showing no FITC-conjugated annexin V- or PI-positive cells; (b) early apoptotic cells (cells only with green fluorescence) with PP-10 at $IC_{50}$ dose after 1.5 h exposure; (c) late apoptotic (cells with both green fluorescence and red-stained cells) at 2 h posttreatment with PP-10; (d) exposure to $IC_{90}$ dose of PP-10 for 3.5 h shows all necrotic cells (red-stained nuclei). Magnification, ×100. (C) Confocal microscopy of PP-10-treated and untreated intracellular amastigotes expressing green fluorescent protein (GFP) from an episomal vector. (a) PP-10-untreated GFP amastigotes show a marked green epifluorescence intensity (upper left) and a merged condition displaying amastigotes within the murine peritoneal macrophages (lower left). (Upper right) Phase-contrast photomicrograph of the GFP parasites retained within the macrophages shown in the upper left panel. (Lower right) Untreated control cells without fluorescence. (b) PP-10 treatment elicited a significant decrease in the green fluorescence of the parasites, leading to death of viable cells (upper and lower left panels). Magnification, ×100. Images are representative of one of three similar results.

imental VL. The lead molecules (PP-9 and PP-10) showed profound antiparasitic activity against both SAG-sensitive and -resistant strains of *Leishmania* in an *in vitro* and as well as an *in vivo* model. PP-9 and PP-10 showed promising leishmanicidal activity with significant $IC_{50}$ doses against intracellular amastigotes of *L. donovani*, with selectivity indexes of 85 and 96, respectively. Therapy with these compounds caused 95 to 98% reductions in spleen and liver parasite burdens with only 4 doses, administered orally to BALB/c mice. PP-9 and PP-10 were more active than miltefosine at similar doses. These lead compounds were devoid of major or visible hepato- and nephrotoxic effects in BALB/c mice. No treatment-related changes in hematology and cardiac function tests (Table 6) were found in PP-9- and PP-10-treated mice. Moreover, electrocardiographic patterns in rats after treatment with PP-10 were normal. The lead compounds were also found to be devoid of mutagenicity and genotoxicity, displaying no evidence of methemoglobinemia even at $IC_{90}$ doses (data not shown). PP-9 and PP-10 were found to be more permeant with oral administration, possessing desirable physicochemical properties, such as moderate lipophilicity and weak basicity, better than even those of miltefosine. Moreover, these compounds were highly stable in liver microsomes. Therefore, there are no chances of oral first-pass metabolism (unpublished data).

Numerous compounds on quinoline scaffolds have previously been reported to be antileishmanials (10). Among these, 2-, 3-, and 4-substituted quinolines were reported to exhibit activity against *L. donovani in vitro* (29, 54). Moreover, two categories of 2-substituted quinoline derivatives were investigated for *in vivo* activity at a 25-mg/kg dose daily for 10 days through the oral route and demonstrated 66% and 69% reductions in liver parasite burden in the murine VL model, respectively (36). Herein, PP-10, a lead compound of the 4-aminoquinaldine series, demonstrated almost complete clearance of the parasites (97% in liver and 98.5% in spleen) from infected BALB/c mice, when treated orally at a dose of 10 mg/kg/week for 1 month. Interestingly, similar results were also reported recently for an 8-aminoquinoline analogue (tafenoquine) (59). It may be noted that whereas Yardley et al. (59) obtained such parasite clearance in a 7-day infection model, our compound (PP-10) cured leishmanial infection in a 2-month-established model of VL with well-expressed hepato- and splenomegaly (41). PP-10, a derivative of S-4, enhanced oral antileishmanial activity significantly over that of the parent compound (47). The augmented effects of PP-10 could be due to the presence of dichloroanilide substituents (38). Thus, PP-11 and PP-13, which lacked a chloroanilide functional group, were devoid of antileishmanial activity, whereas PP-2,

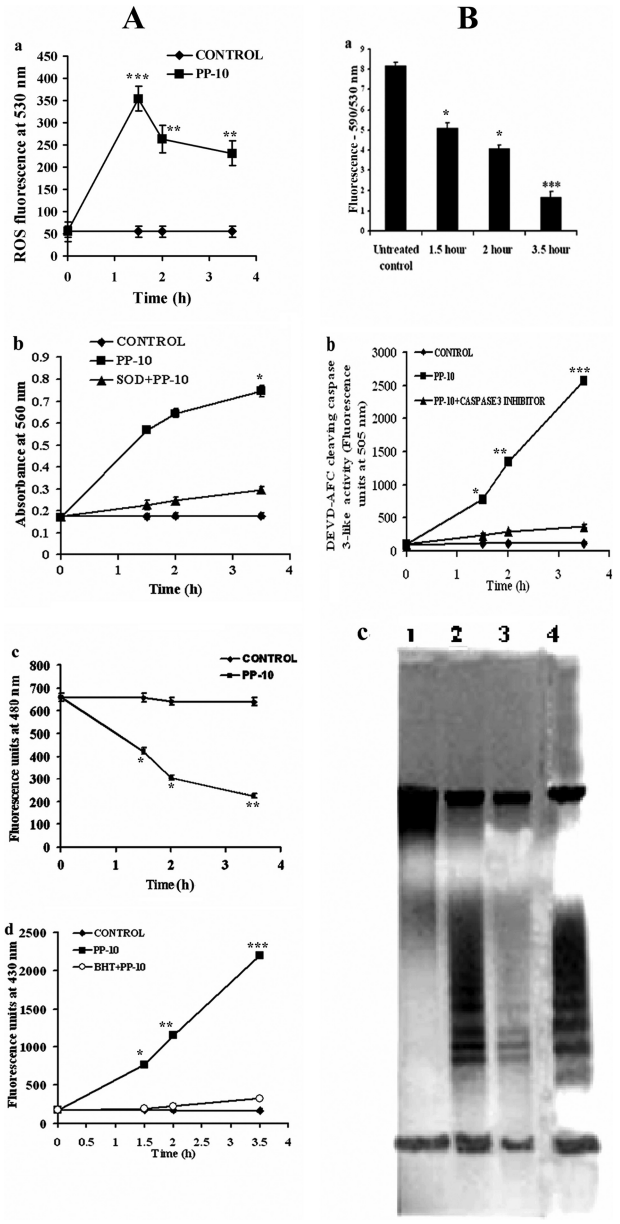


**FIG 3** PP-10-induced apoptotic cell death cascade in *L. donovani* promastigotes. (A) (a) Production of intracellular superoxide radicals was measured after treatment of AG83 promastigotes with $IC_{50}$ dose of PP-10. (b) Generation of hydroxyl radicals was measured after treatment at $IC_{50}$ dose of PP-10. The level of superoxide radicals was also determined after addition of the antioxidant SOD to PP-10-treated cells. (c) The intracellular GSH level in *L. donovani* promastigotes was measured after treatment with PP-10 at $IC_{50}$ dose. (d) The level of fluorescent products of lipid peroxidation was estimated after treatment with PP-10 at $IC_{50}$ dose with and without BHT. (B) (a) Effect of treatment of PP-10 at $IC_{50}$ dose on the mitochondrial membrane potential of AG83 promastigotes using JC-1 fluorescence. (b) Activation of protease of the CED3/CPP32 group inside leishmanial cells was measured after treatment with $IC_{50}$ dose of PP-10 and in the presence or absence of protease inhibitor. (a and b) Data represent the mean ± SEM of three independent experiments. Data with *P* values of <0.0001 (***), <0.001 (**), and <0.05 (*) were considered statistically significantly different compared to the 0.02% DMSO control, assessed by the unpaired Student *t* test. (c) Fragmentation of genomic DNA in the presence of PP-10 compared to untreated control cells. Genomic DNA was isolated from AG83 promastigotes after treatment with 0.2% DMSO alone (lane 1) or $IC_{50}$ dose of PP-10 for 3.5 h (lane 2) and 2 h (lane 3) and promastigotes treated with 5 mM camptothecin for 3.5 h as a positive control (lane 4).

PP-9, and PP-10, having chloro- and dichloroanilide substituents, displayed significant oral antileishmanial activity in established VL.

Preliminary investigations reported earlier (47) that S-4, the parent compound of our 4-aminoquinaldine series, mediated leishmanicidal activity through cell cycle arrest, indicating apoptosis. Therefore, in this study, we investigated in detail the killing mode of PP-10 on *L. donovani* promastigotes to unravel its remarkable antileishmanial activity. PP-10 was chosen for elucidation of the mechanism of action, since it had the lowest $IC_{50}$ against promastigotes and the strongest efficacy against intracellular amastigotes. Promastigotes treated with PP-10 demonstrated round parasites with increases in vacuoles, granules, and lipid bodies. Moreover, cell shrinkage, loss of plasma membrane integrity along with blebbing, chromatin condensation, and dilation of mitochondria, hallmarks of apoptotic cell death (51), were observed. Lack of extensive round lysosome-like cytoplasmic intracellular vacuoles, chromatin condensation, and the absence of intact plasma membrane with insignificant cell shrinkage and swelling, along with insignificant changes in nuclear and mitochondrial integrity, observed herein, are indicative of apoptotic rather than autophagic cell death (50). Further, increases in annexin V positivity and intracellular ROS generation, upregulation of hydroxyl radicals, downregulation of GSH levels, elevation of lipid peroxide levels, a decrease in mitochondrial membrane potential, and elevation of late-stage apoptosis markers such as protease activation and DNA nucleosomal fragmentation in the treated promastigotes support induction of apoptosis-like PCD (20).

While the above-described results support our proposed mechanism of action at a cellular level, identification of a suitable drug target in the parasite would be an efficient approach for development of safe antiparasitic lead compounds (37). DHFR is a key regulatory cellular enzyme of folate metabolism. Inhibition of DHFR leads to cell death through a lack of thymine (nucleotide metabolism) (31, 45). The structural similarity of our compounds with the reported DHFR inhibitors (5, 23) prompted us to carry out molecular docking studies of the three major lead compounds of our series with leishmanial DHFR to elucidate their structure-based mechanism. Docking results illustrated that the leads were mild to moderate inhibitors of leishmanial DHFR, and this finding was validated by an experimental *in vitro* spectrophotometric DHFR inhibition assay, indicating an activity trend of PP-10 > PP-9 > PP-2. Docking scores matched the experimental results. Recent studies (31, 60) on *L. donovani chagasi* DHFR revealed that their DHFR binding site is identical to that of *L. major* DHFR and the protein-ligand interaction pattern is conserved in both species, suggesting that *L. major* DHFR can be used as a surrogate model for *L. donovani* DHFR-targeted drug discovery. However, whether this inhibition is linked with PP-10-induced PCD or not is not clear. DHFR inhibition upregulates generation of intracellular ROS and triggering of the endonucleolytic fragmentation of DNA, which contribute to the induction of apoptosis-mediated cell death in eukaryotic cells (3, 27, 39). We may therefore postulate that PP-10 may kill *Leishmania* parasites through a similar mechanism involving inhibition of leishmanial DHFR, followed by apoptosis-mediated PCD (21, 43). Since these findings were based on only 3 lead compounds, further studies with more analogs of this series would be required to prove the hypothesis that compounds which do not inhibit DHFR also fail to induce apoptosis.

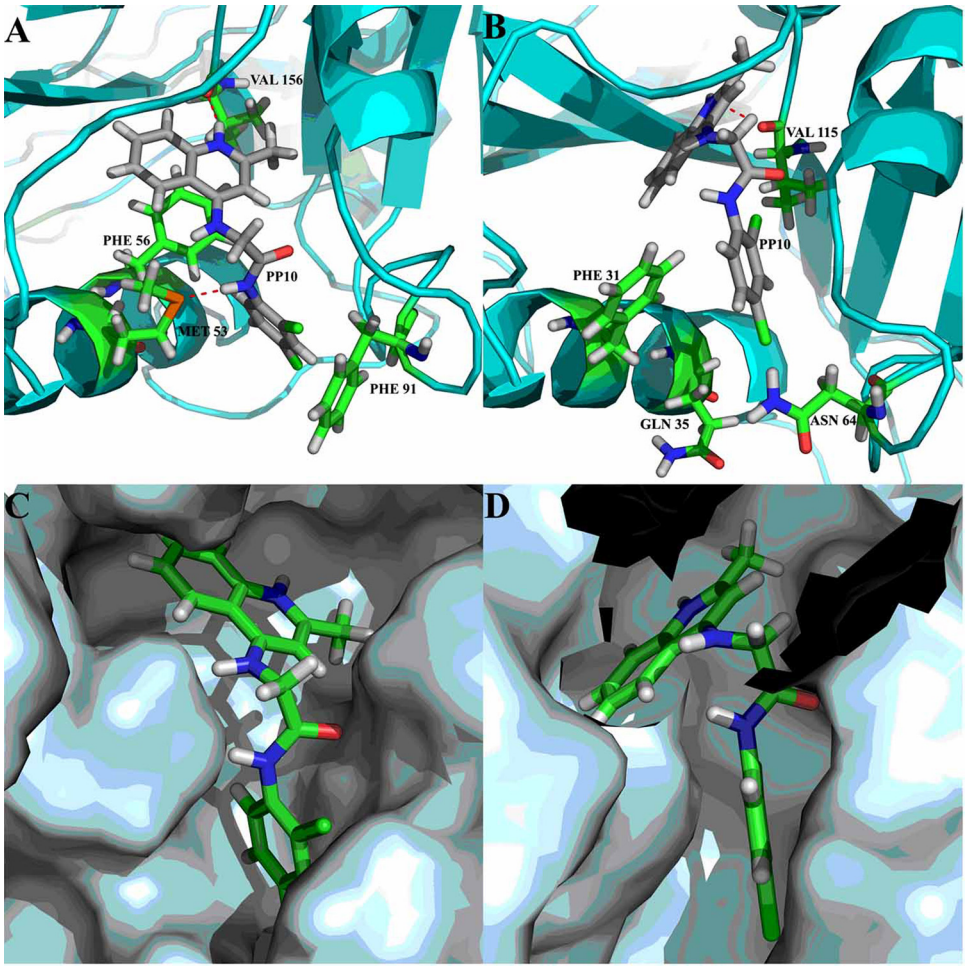


**FIG 4** Docked binding mode of PP-10 depicting its nonbonded interaction. (A and B) The active-site residues are rendered in stick representation. Interaction with *L. major* DHFR (A) represents the interactions with human DHFR (B). (C and D) Binding mode of PP-10 to *L. major* DHFR and human DHFR, respectively. Some of the binding-site residues in panel C are hidden for clarity.

A lack of safe and orally effective antileishmanial drugs, coupled with emerging drug resistance and high treatment costs, makes the therapy of VL difficult (13). The only oral drug, miltefosine, suffers from drawbacks, such as gastrointestinal and reproductive toxicity, recrudescence of leishmanial infection posttreatment, a long biological half-life (100 to 200 h), and a low therapeutic index (34). In this scenario, the efficacy of PP-9 and PP-10 against SAG-sensitive and -resistant parasites for oral treatment of experimental VL is remarkable. The high permeation of PP-9 and PP-10, which may promote a higher rate of absorption in the systemic circulation through passive diffusion, could be responsible for the antileishmanial activity of PP-9 and PP-10 through the oral route. Furthermore, since PP-10 has a binding capacity of 46.5% with human plasma proteins (data not shown), it is expected that PP-10 may also have a short biological half-life, thus avoiding the problem of resistance development often associated with drugs having prolonged biological half-lives (52). Further *in vivo* pharmacokinetic studies are in progress with PP-9 and PP-10 to explore their oral therapeutic potential to combat this neglected disease. In conclusion, PP-9 and PP-10 are promising preclinical development candidates for oral drug therapy for VL, alone or in combination with currently used antileishmanials,

**TABLE 6** Serum clinical chemistry evaluations after 4 repeat dose administrations in mice[a]

| Compound | Dose (mg/kg) | Concn (IU/liter) | | | Concn (mg/dl) | | Concn (U/liter) | | Cholesterol concn (mg/dl) |
|---|---|---|---|---|---|---|---|---|---|
| | | SGPT | SGOT | ALP | Urea | Creatinine | LDH | CK-MB | |
| Vehicle | 0 | 28 (7) | 71 (5) | 38 (2) | 29 (6) | 12 (2) | 630 (39) | 120 (12) | 124 (18) |
| PP-9 | 10 | 30 (6) | 65 (7) | 40 (3) | 30 (4) | 11 (1) | 620 (40) | 78 (9) | 115 (12) |
| PP-10 | 10 | 28 (4) | 72 (2) | 39 (4) | 31 (3) | 14 (0.678) | 625 (29) | 118 (11) | 128 (9) |

[a] All compounds were administered orally. Values are means (standard deviations) of four animals. SGPT, serum glutamate pyruvate transaminase; SGOT, serum glutamate oxaloacetate transaminase; ALP, alkaline phosphatase; LDH, lactate dehydrogenase; CK-MB, creatine kinase.

with prospects also for rescue treatment of antimony treatment failure.

## ACKNOWLEDGMENTS

This work was supported by grants from Indian Council Medical Research, government of India.

We thank Manjarika De, Janmenjay Midya, and Neeloo Singh for parasite culture, performing animal experiments, and the GFP *Leishmania* strain.

We do not have a commercial or other association that might pose a conflict of interest.

## REFERENCES

1. **Afrin F, Ali N.** 1997. Adjuvanticity and protective immunity elicited by Leishmania donovani antigens encapsulated in positively charged liposomes. Infect. Immun. **65**:2371–2377.
2. **Ameisen JC.** 2002. On the origin, evolution, and nature of programmed cell death: a timeline of four billion years. Cell Death Differ. **9**:367–393.
3. **Backus HH, et al.** 2003. Thymidylate synthase inhibition triggers apoptosis via caspases-8 and -9 in both wild-type and mutant p53 colon cancer cell lines. Eur. J. Cancer **39**:1310–1317.
4. **Banki K, Hutter E, Gonchoroff NJ, Perl A.** 1999. Elevation of mitochondrial transmembrane potential and reactive oxygen intermediate levels are early events and occur independently from activation of caspases in Fas signaling. J. Immunol. **162**:1466–1479.
5. **Berman JD, King M, Edwards N.** 1989. Antileishmanial activities of 2,4-diaminoquinazoline putative dihydrofolate reductase inhibitors. Antimicrob. Agents Chemother. **33**:1860–1863.
6. **Bermudez R, Dagger F, D'Aquino JA, Benaim G, Dawidowicz K.** 1997. Characterization of mitochondrial electron-transfer in Leishmania mexicana. Mol. Biochem. Parasitol. **90**:43–54.
7. **Chakrabarti G, et al.** 1999. Indolylquinoline derivatives are cytotoxic to Leishmania donovani promastigotes and amastigotes in vitro and are effective in treating murine visceral leishmaniasis. J. Antimicrob. Chemother. **43**:359–366.
8. **Chappuis F, et al.** 2007. Visceral leishmaniasis: what are the needs for diagnosis, treatment and control? Nat. Rev. **5**:873–882.
9. **Chowdhury AR, et al.** 2003. Dihydrobetulinic acid induces apoptosis in Leishmania donovani by targeting DNA topoisomerase I and II: implications in antileishmanial therapy. Mol. Med. **9**:26–36.
10. **Croft SL, Seifert K, Yardley V.** 2006. Current scenario of drug development for leishmaniasis. Indian J. Med. Res. **123**:399–410.
11. **Das M, Mukherjee SB, Shaha C.** 2001. Hydrogen peroxide induces apoptosis-like death in Leishmania donovani promastigotes. J. Cell Sci. **114**:2461–2469.
12. **Das R, Roy A, Dutta N, Majumder HK.** 2008. Reactive oxygen species and imbalance of calcium homeostasis to curcumin induced programmed cell death in *Leishmania donovani.* Apoptosis **13**:867–882.
13. **Davis AJ, Kedzierski L.** 2005. Recent advances in antileishmanial drug development. Curr. Opin. Investig. Drugs **6**:163–169.
14. **Deb I, et al.** 2009. Synthesis and characterizations of novel quinoline derivatives having mixed ligand activities at the kappa and mu receptors: potential therapeutic efficacy against morphine dependence. Bioorg. Med. Chem. **17**:5782–5790.
15. **Dey T, Anam K, Afrin F, Ali N.** 2000. Antileishmanial activities of stearylamine-bearing liposomes. Antimicrob. Agents Chemother. **44**: 1739–1742.
16. **Dubar F, Khalife J, Brocard J, Dive D, Biot C.** 2008. Ferroquine, an ingenious antimalarial drug: thoughts on the mechanism of action. Molecules **13**:2900–2907.
17. **Duranteau J, Chandel NS, Kulisz A, Shao Z, Schumacker PT.** 1998. Intracellular signaling by reactive oxygen species during hypoxia in cardiomyocytes. J. Biol. Chem. **273**:11619–11624.
18. **Fairlamb AH, Cerami A.** 1992. Metabolism and functions of trypanothione in the Kinetoplastida. Annu. Rev. Microbiol. **46**:695–729.
19. **Galvao LO, et al.** 2000. Therapeutic trial in experimental tegumentary leishmaniasis caused by Leishmania (Leishmania) amazonensis. A comparative study between mefloquine and aminosidine. Rev. Soc. Bras. Med. Trop. **33**:377–382.
20. **Gamcsik MP, et al.** 2001. Dual role of glutathione in modulating camptothecin activity: depletion potentiates activity, but conjugation enhances the stability of the topoisomerase I-DNA cleavage complex. Mol. Cancer Ther. **1**:11–20.

20a. **Hidalgo IT, et al.** 1989. Characterization of the human colon carcinoma cell line (Caco-2) as a model system for intestinal epithelial permeability. Gastroenterology **96**:736–749.

21. **Ian HG.** 2002. Inhibitors of dihydrofolate reductase in *Leishmania* and trypanosomes. Biochim. Biophys. Acta **1587**:249–257.
22. **Jha TK, et al.** 1999. Miltefosine, an oral agent, for the treatment of Indian visceral leishmaniasis. N. Engl. J. Med. **341**:1795–1800.
23. **Johnson JV, Rauchman BS, Baccanari DP, Roth B.** 1989. 2,4-Diamino-5-benzylpyrimidines and analogues as antibacterial agents. 12. 1,2-Dihydroquinolylmethyl analogues with high activity and specificity for bacterial dihydrofolate reductase. J. Med. Chem. **32**:1942–1949.
24. **Khabnadideh S, et al.** 2005. Design, synthesis and evaluation of 2,4-diaminoquinazolines as inhibitors of trypanosomal and leishmanial dihydrofolate reductase. Bioorg. Med. Chem. **13**:2637–2649.
25. **Knighton DR, et al.** 1994. Structure of and kinetic channelling in bifunctional dihydrofolate reductase-thymidylate synthase. Nat. Struct. Biol. **1**:186–194.
26. **Kono Y.** 1978. Generation of superoxide radical during autoxidation of hydroxylamine and an assay for superoxide dismutase. Arch. Biochem. Biophys. **186**:189–195.
27. **Kwok JB, Tattersall MH.** 1992. DNA fragmentation, dATP pool elevation and potentiation of antifolate cytotoxicity in L1210 cells by hypoxanthine. Br. J. Cancer **65**:503–508.
28. **Lee N, et al.** 2002. Programmed cell death in the unicellular protozoan parasite Leishmania. Cell Death Differ. **9**:53–64.
29. **Loiseau PM, et al.** 2011. In vitro activities of new 2-substituted quinolines against Leishmania donovani. Antimicrob. Agents Chemother. **55**: 1777–1780.
30. **Lopez-Martin C, Perez-Victoria JM, Carvalho L, Castanys S, Gamarro F.** 2008. Sitamaquine sensitivity in Leishmania species is not mediated by drug accumulation in acidocalcisomes. Antimicrob. Agents Chemother. **52**:4030–4036.
31. **Maganti L, Manoharan P, Ghoshal N.** 2010. Probing the structure of Leishmania donovani chagasi DHFR-TS: comparative protein modeling and protein-ligand interaction studies. J. Mol. Model. **16**:1539–1547.
32. **Majumder S, Dey SN, Chowdhury R, Dutta C, Das J.** 1988. Intracellular development of cholerphage Φ149 under permissive and nonpermissive conditions: an electron microscopic study. Intervirology **29**:27–38.
33. **Mishra BB, Singh RK, Srivastava A, Tripathi VJ, Tiwari VK.** 2009. Fighting against Leishmaniasis: search of alkaloids as future true potential anti-leishmanial agents. Mini Rev. Med. Chem. **9**:107–123.
34. **Mishra J, Saxena A, Singh S.** 2007. Chemotherapy of leishmaniasis: past, present and future. Curr. Med. Chem. **14**:1153–1169.
35. **Mosmann T.** 1983. Rapid colorimetric assay for cellular growth and survival: application to proliferation and cytotoxicity assays. J. Immunol. Methods **65**:55–63.
36. **Nakayama H, et al.** 2005. Efficacy of orally administered 2-substituted quinolines in experimental murine cutaneous and visceral leishmaniases. Antimicrob. Agents Chemother. **49**:4950–4956.
37. **Nare B, Hardy LW, Beverley SM.** 1997. The roles of pteridine reductase 1 and dihydrofolate reductase-thymidylate synthase in pteridine metabolism in the protozoan parasite Leishmania major. J. Biol. Chem. **272**: 13883–13891.
38. **Naumann K.** 2000. Influence of chlorine substituents on biological activity of chemicals: a review. Pest Manag. Sci. **56**:3–21.
39. **Navarro-Peran E, et al.** 2005. The antifolate activity of tea catechins. Cancer Res. **65**:2059–2064.
40. **Nwaka S, Hudson A.** 2006. Innovative lead discovery strategies for tropical diseases. Nat. Rev. Drug Discov. **5**:941–955.
41. **Pal S, Ravindran R, Ali N.** 2004. Combination therapy using sodium antimony gluconate in stearylamine-bearing liposomes against established and chronic Leishmania donovani infection in BALB/c mice. Antimicrob. Agents Chemother. **48**:3591–3593.
42. **Pecoul B.** 2004. New drugs for neglected diseases: from pipeline to patients. PLoS Med. **1**:e6.
43. **Peters GJ, et al.** 2000. Molecular downstream events and induction of thymidylate synthase in mutant and wild-type p53 colon cancer cell lines after treatment with 5-fluorouracil and the thymidylate synthase inhibitor raltitrexed. Eur. J. Cancer **36**:916–924.
44. **Peters W.** 1981. The treatment of kala-azar—new approaches to an old problem. Indian J. Med. Res. **73**(Suppl):1–18.

45. **Renslo AR, McKerrow JH.** 2006. Drug discovery and development for neglected parasitic diseases. Nat. Chem. Biol. **2**:701–710.
46. **Rodenhuis S, Kremer JM, Bertino JR.** 1987. Increase of dihydrofolate reductase in peripheral blood lymphocytes of rheumatoid arthritis patients treated with low-dose oral methotrexate. Arthritis Rheum. **30**:369–374.
47. **Sahu NP, et al.** 2002. Synthesis of a novel quinoline derivative,2-(2-methylquinolin-4-ylamino)-N-phenylacetamide—a potential antileishmanial agent. Bioorg. Med. Chem. **10**:1687–1693.
48. **Savioli L, et al.** 2006. Response from Savioli and colleagues from the Department of Neglected Tropical Diseases, World Health Organization. PLoS Med. **3**:e283.
49. **Schlegel RA, Williamson P.** 2001. Phosphatidylserine, a death knell. Cell Death Differ. **8**:551–563.
50. **Schurigt U, et al.** 2010. Aziridine-2,3-dicarboxylate-based cysteine cathepsin inhibitors induce cell death in Leishmania major associated with accumulation of debris in autophagy-related lysosome-like vacuoles. Antimicrob. Agents Chemother. **54**:5028–5041.
51. **Sen N, et al.** 2004. Camptothecin induced mitochondrial dysfunction leading to programmed cell death in unicellular hemoflagellate Leishmania donovani. Cell Death Differ. **11**:924–936.
52. **Shargel L, Wu-Pong S, Yu ABC.** 2005. Applied biopharmaceutics & pharmacokinetics. Appleton & Lange Reviews/McGraw-Hill, Medical Publishing Division, New York, NY.
53. **Shimasaki H.** 1994. Assay of fluorescent lipid peroxidation products. Methods Enzymol. **233**:338–346.
54. **Tempone AG, et al.** 2005. Synthesis and antileishmanial activities of novel 3-substituted quinolines. Antimicrob. Agents Chemother. **49**:1076–1080.
55. **Vijayan RS, Prabu M, Mascarenhas NM, Ghoshal N.** 2009. Hybrid structure-based virtual screening protocol for the identification of novel BACE1 inhibitors. J. Chem. Infect. Model. **49**:647–657.
56. **West JA, et al.** 2000. Heterogeneity of Clara cell glutathione. A possible basis for differences in cellular responses to pulmonary cytotoxicants. Am. J. Respir. Cell Mol. Biol. **23**:27–36.
57. **World Health Organization.** 1999. Tropical disease research: progress in international research, 1997-1998. World Health Organization, Geneva Switzerland.
58. **World Health Organization.** 2010. Leishmaniasis: burden of disease. World Health Organization, Geneva, Switzerland. http://www.who.int/leishmaniasis/burden/en.
59. **Yardley V, Gamarro F, Croft SL.** 2010. Antileishmanial and antitrypanosomal activities of the 8-aminoquinoline tafenoquine. Antimicrob. Agents Chemother. **54**:5356–5358.
60. **Zuccotto F, Martin AC, Laskowski RA, Thornton JM, Gilbert IH.** 1998. Dihydrofolate reductase: a potential drug target in trypanosomes and leishmania. J. Comput. Aided Mol. Des. **12**:241–257.